Facile strategy toward the development of a self-healing coating by electrospray method

Mohammad Sadegh Koochaki [1,2], Saied Nouri Khorasani [1,*], Rasoul Esmaeely Neisiany [3,4], Ali Ashrafi [5], Mirko Magni [2] and Stefano P. Trasatti [2]

[1] Department of Chemical Engineering, Isfahan University of Technology, Isfahan, 84156-83111, Iran

[2] Department of Environmental Science and Policy, Università degli Studi di Milano, Milan 20133, Italy

[3] Department of Materials and Polymer Engineering, Hakim Sabzevari University, Sabzevar, 9617976487, Iran

[4] Division of Materials Science, Department of Engineering Sciences and Mathematics, Luleå University of Technology, SE-97187 Luleå, Sweden

[5] Department of Material Engineering, Isfahan University of Technology, Isfahan, 84156-83111, Iran

***Corresponding author's email: saied@cc.iut.ac.ir**

Abstract:

A self-healing anti-corrosion epoxy coating was prepared by the incorporation of dual capsule healing system. Microcapsules were prepared through the facile electrospray method by using Poly(styrene-co-acrylonitrile) polymer as shell material. Polyetheramine and Methylene diphenyl diisocyanate (MDI) based isocyanate prepolymer were utilized as core materials because of their high reactivity and low sensitivity in forming polyurea polymers. scanning electron microscopy (sem) images confirmed the spherical morphology of the prepared microcapsules with average diameters of 0.93±0.55 µm and 1.21±0.68 µm for the encapsulated polyetheramine and isocyanate microcapsules, respectively. Moreover, transmission electron microscope (TEM), Fourier Transform Infrared spectroscopy (FTIR), and thermogravimetric analysis (TGA) results confirmed the successful encapsulation of both core materials with a high encapsulation yield (71% and 68% for Polyetheramine and

MDI based isocyanate respectively). Electrochemical impedance spectroscopy (EIS) and potentiodynamic polarization technique were used to assess the effects of utilizing the aforementioned system on the intrinsic anti-corrosion barrier property (on pristine samples) and the self-healing efficiency (after cross scratching) of the resulting smart coatings. The corrosion assessment results confirmed the self-healing performance of the incorporated capsules along with a high healing efficiency (85%) for the optimum microcapsule content.

Keywords: self-healing; coatings; electrospray; encapsulation; epoxy.

1. Introduction

The global cost of corrosion was estimated to be 3.4% of the gross domestic product (GDP) [1]. Therefore, employing effective and economical methods is crucial for minimizing corrosion phenomena. Cathodic protection, using corrosion-resistant materials and barrier protection have known as the most popular methods [2]. Among these methods, the organic anti-corrosion paints and coatings which act as barriers against water and oxygen have been widely used due to their effectiveness, low cost and facility to apply [3-6]. These coatings are mostly made of polymeric matrixes known as the “binder” and solid functional additives, commonly known as “pigments”. The main problem with these coatings is that their polymeric matrix can undergo damages by external factors such as mechanical, thermal, chemical, radiation, or a combination of them [7]. These factors lead to the formation of microcracks that can propagate and initiate a catastrophic failure in the coating performance. Detection and repair of these microcracks with conventional methods are time and cost consuming and in many cases impossible [8]. Several solutions have been proposed to overcome this issue. Using self-healing systems, which can restore the original integrity and repair the performance spontaneously without the need for diagnosis or intervention, has

gained a lot of attention in the last two decades [9-11]. Self-healing systems are classified into extrinsic and intrinsic categories according to the healing mechanism [12-14]. Extrinsic self-healing materials do not have the inherent ability to repair themselves and the healing process is done by releasing the healing agents from external reservoirs which are embedded in the matrix. Several strategies have been proposed to develop the extrinsic self-healing materials, considering the release of the healing agent has been shown the most particular performance. Micro/nano capsules, hollow fibers, and vascular systems are the most used reservoirs in extrinsic self-healing [7, 15]. So far, the extrinsic microcapsule-based approach has shown high healing efficiency in many systems [16].

Several kinds of active reagents including dicyclopentadiene (DCPD), polydimethylsiloxane (PDMS), glycidyl methacrylate, isocyanates, drying oils, epoxy resin, and amines have been successfully employed as an extrinsic healing agent [17-19]. Researches have shown that the activity and stability of the healing agents are critical to the healing reaction efficiency as well as the environmental conditions during the reaction [7]. However, most of the reported systems have demonstrated their self-healing ability at standard laboratory temperature/humidity conditions. Therefore, the development of a self-healing system with excellent performance even in unconventional conditions is still a major challenge [20].

On the other hand, *in situ* polymerization, interfacial polymerization, internal phase separation, and Pickering emulsion technique are some of the methods used for encapsulating the healing agents [21-24]. It should be noted that these encapsulation techniques are very sensitive, hard to control, expensive and mostly not eco-friendly. The use of low-cost lab-made electrospinning/ electrospraying techniques can open up a promising future for encapsulation purposes [25-27]. The electrospinning technique was first used for making hollow fibers as containers in vascular self-healing systems [28, 29]. Although several vascular-based self-healing composites with different core and shell materials have

been reported using this method, their production process is sophisticated and their application in paint and coatings is not possible [30-32]. Production of micro/nano particles through the electrospray method has been studied before in the agriculture, food and drug delivery but Hia and coworkers reported, firstly, the usage of this technology in producing microcapsules containing epoxy resin-based healing agent within the alginate shell for self-healing application [33].

In this research, the self-healing performance of a dual capsule self-healing system based on polyurea formation stepwise polymerization is studied in an epoxy matrix to develop a robust and efficient self-healing anti-corrosion coating. The nucleophilic reaction between amines and isocyanates forming polyurea polymers is selected as a healing system due to its great potential even in the unconventional environmental conditions [34]. This reaction does not need any catalysts and can occur directly at low temperatures, high humidity and even in the presence of water [35, 36]. Furthermore, the healing agents are encapsulated in Poly(styrene-co-acrylonitrile) (SAN) by a continuous, simple, easy to control and cost-efficient electrospray method.

2. Materials and Methods

2.1. Materials

SAN with a molecular weight of 185,000 Da and 30 wt% acrylonitrile content was used as the capsules shell material. Dimethylformamide (DMF) solvent was employed for the preparation of uniform polymer solutions. Both of the SAN and DMF were purchased from Sigma-Aldrich. The healing agents (core materials) in the dual capsule system were chosen as follows. Poly(propylene glycol) bis(2-aminopropyl ether) with a molecular weight of 230, known as Jeffamine™ D 230, was purchased from Huntsman. CORONATE™ 1391, a low viscosity polymeric isocyanate based on 4,4’-diphenylmethane diisocyanate with average

isocyanate group content of 32% was provided by TOSOH Corporation. The self-healing performance of the mentioned healing system was studied in an epoxy coating which was prepared from materials and procedures specified in previous work [19].

2.2. Preparation of the capsules.

The SAN solution in DMF (4% w/v) was prepared by mixing the adequate amount of SAN powder at room temperature for 24 h using a magnetic stirrer at 60 rpm. Subsequently, amine and isocyanate, which act as core materials, were added to separate vials of this solution and kept the stirring in the same conditions for 2 more h followed by 20 minutes of sonication in a sonicator bath. The core/shell weight ratio was adjusted at 0.5 w/w for both solutions. The resulted solutions were then transferred to the injection syringes and pumped (SP102- Fnm co. Ltd.) separately with a flow rate of 0.3 mL/h through a G23 stainless steel needle.

A DC potential in the range of 22–26 kV was applied between the needle and the collector, while the last being set as ground. During the electrospray process, microcapsules were formed through the solvent evaporation of the solution in their path from the needle tip to the collector. The distance between the needle tip and the collector was set 15cm. Two separate watch glasses containing diluted epoxy resin (EPON 828R mixed with ED180 in 3:1 weight ratio) and polyaminoamide hardener were placed on top of a conductive ground plate to collect isocyanate and amine capsules, respectively. It should be noted that for characterization of the capsules they were directly collected on the grounded aluminum foil sheets. Figure 1 schematically illustrates the above-mentioned electrospray setup.

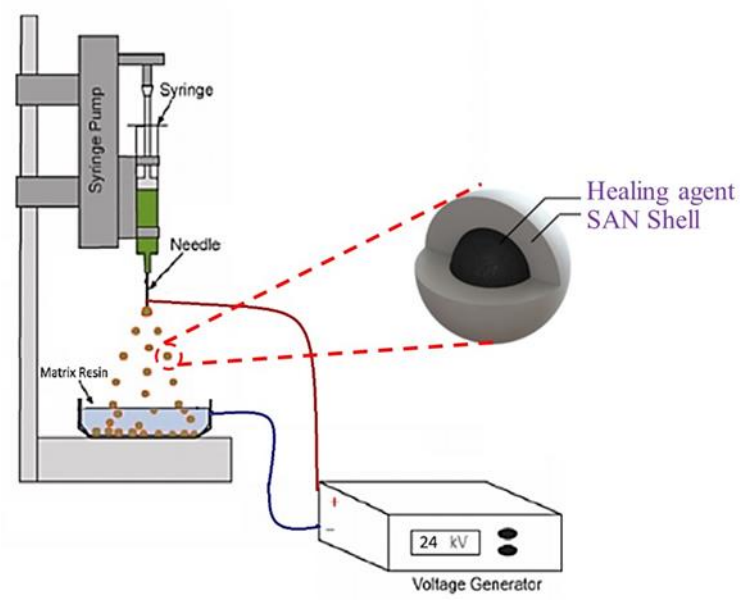

Figure 1. The schematic illustration of employed electrospray set up for the preparation of core-shell capsules.

2.3. Preparation of self-healing anti-corrosion coatings

First, the epoxy resin and its corresponding curing agent containing the microcapsules, obtained from the previous step, were stirred mechanically to ensure proper dispersion (200 rpm for 5 minutes). Then the above-mentioned components of the coating were mixed together with a 2:1 (epoxy:curing agent) mass ratio at ambient temperature prior to coatings application. The total microcapsule content of the final mixtures containing the two types of microcapsules was varied from 1 to 6 percent by weight, while the ratio of amine and isocyanate-containing microcapsules was kept at 1:1 by weight.

Several pieces of bare steel panels (Q-PANEL) were polished with 400 grit sandpaper followed by washing with acetone for degreasing. Afterward, each dried panel was coated with a 100 µm thickness epoxy-based coating using a universal film applicator (ZEHTNER ZAU 2000.80). The coating was cured at room temperature for 7 days. After 7 days, the coatings were scratched manually by a scalpel cutter for further corrosion tests. Coatings were kept at room temperature in the lab for 7 days before testing to allow the probable

healing of capsule containing samples. The control sample was prepared with the same procedure without microcapsule incorporation.

2.4. Characterization

2.4.1. Characterization of the prepared capsules

The size, size distribution, and morphology of the collected capsules were studied by a scanning electron microscopy (JEOL JSM-5500 LV Scanning Electron Microscope, JEOL, Japan). The surfaces of the samples were coated by gold plasma sputtering before SEM analysis. Size distributions were obtained and calculated by Image J analysis software using 50 measurements. Moreover, a dynamic light scattering (DLS) technique was used to investigate the size distribution of the prepared microcapsules. The studies were carried out in a liquid medium using Nanopartica SZ-100; HORIBA, Japan apparatus. In order to a better dispersion, the microcapsules were firstly dispersed in methanol by ultrasonic homogenizer (Q500 Sonicator, Qsonica, USA) for 30 minutes before the testing. The tests were performed at 90 degrees.

In addition, Transmission electron microscopy (LEO 912ab Energy Filtering TEM model operated at 120kv, Zeiss, Germany) was employed to confirm the core-shell structure of the prepared capsules. The capsules were directly electrosprayed onto a Lacey Formvar/carbon-coated copper grid for TEM analysis.

Fourier-transform infrared spectroscopy (Perkin-Elmer Spectrum 100 FTIR spectrometer) was used in the range of 4000–400 cm^{-1} to investigate the chemical components of core and shell materials as well as the successful encapsulation without any chemical reactions.

To determine the core content and thermal stability of the prepared capsules, Thermogravimetric analysis (TGA/DSC 2 STAR- Mettler-Toledo – Switzerland) was employed under a nitrogen atmosphere from 25 °C to 500 °C at a heating rate of 10 °C/min.

2.4.2. Electrochemical characterization of the coatings

To evaluate the anti-corrosion properties and self-healing ability of the aforementioned system, The prepared coatings including capsule-containing and the control samples were studied via Electrochemical Impedance Spectroscopy (EIS) and potentiodynamic polarization analyses. The cracked coatings were exposed to a simplified seawater model constituted by a naturally aerated near-neutral 3.5 wt.% NaCl solution (≥ 99.0%, Sigma-Aldrich) in MilliQ® water for 14 days before testing; each sample was monitored by recording EIS spectra at fix interval times. According to the fact that the self-healing process is conducted via an extrinsic system, the effect of the added microcapsules on the barrier property of the resulting coatings was also studied by potentiodynamic polarization analysis after 7 days of exposure to the aforementioned 3.5 wt.% NaCl solution. It should be noted that in this case the coatings had no cracks and the microcapsules are present in the matrix just as fillers. The tests were conducted by an Interface 1000 potentiostat (Gamry) in a home-made three-electrode cell with the coated metals, employed as a working electrode, attached to the bottom of the cell. The sample was exposed to the inner solution through a circular hole in the bottom of the cell (geometric area 0.785 cm^2). A platinum rod and aqueous saturated calomel electrode (SCE), have been employed as the counter and reference electrode, respectively. A Luggin capillary was used to minimize the ohmic drop between the working electrode and the reference one. .

The potentiostatic measurements were obtained at the open circuit potential (OCP) within a frequency range from 10^5 to 10^{-2} Hz with a logarithmically distributed sweeping frequency of 10 points per decade, using a sinusoidal voltage of 10 mV in amplitude. The potentiodynamic polarization curves were recorded from -0.3 V to +0.3 V *vs.* OCP at 0.167 mV s^{-1} scan rate.

3. Results and Discussions

3.1. Morphology and size distribution of the capsules

Figure 2a represents the SEM micrograph of the capsules containing amine which were sprayed at 15 cm distance (24 kV, 0.3 $mlhr^{-1}$), with 33 wt.% initial core material content. It can be observed that the prepared capsules are spherical in shape with a rough outer shell wall. Similarly, Figure 3a shows the SEM image of the prepared capsules containing isocyanate, at the same process conditions. The diameters of the microcapsules were measured by ImageJ software at least 50 times to plot the size distribution diagram (Figures 2b and 3b) by Prism software. As shown in ~~the~~ Figures 2b and 3b, the diameter of obtained microcapsules in both cases was less than 3 microns, with the highest frequency in the range of 500 to 1000 nm. The average particle size in the amine and isocyanate-containing microcapsules was to be 0.93 µm and 1.21 µm, respectively. Moreover, the size distribution and average particle size of both microcapsules were studied by DLS technique in a liquid medium and the results are shown in Figures S1 and S2. The DLS results confirm that the microcapsules were completely dispersed in methanol without any sign of clusters or agglomeration.

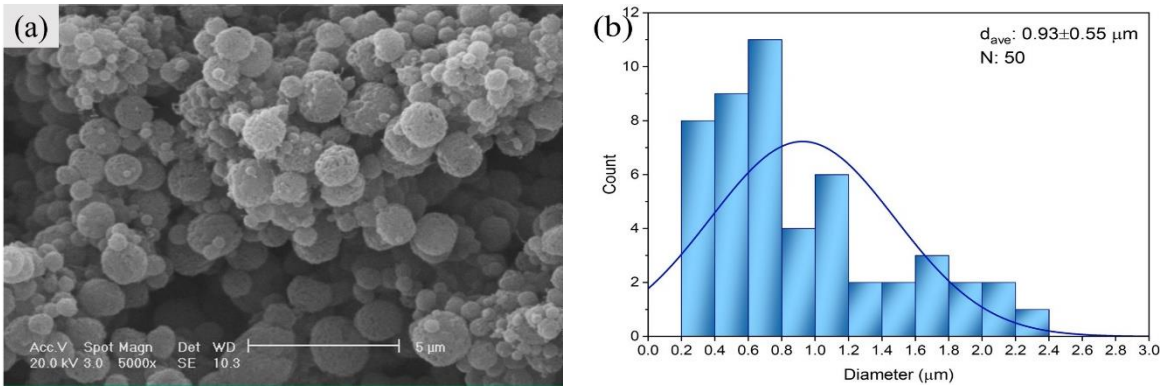

Figure 2. (**a**) SEM images of the capsules containing amine; (**b**) Size distribution diagram of the amine-containing capsules.

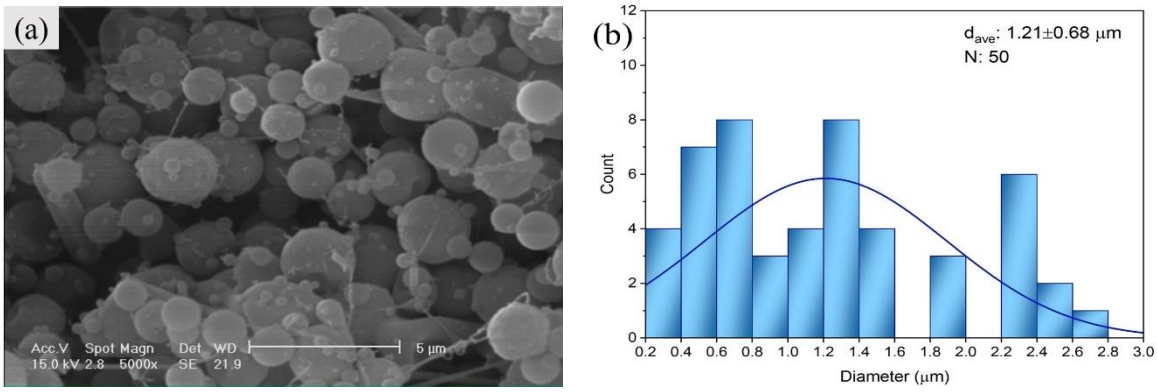

Figure 3. (**a**) SEM images of the capsules containing Isocyanate; (**b**) Size distribution diagram of the isocyanate- containing capsules.

Figure 4 represents the TEM images of the electrosprayed microcapsules. It can be discerned that the core-shell structure was formed for both types of microcapsules. Furthermore, there is a uniform gray core in isocyanate-containing microcapsules, while the multicore structure was formed in the amine-containing ones. A similar structure was reported by Hia and coworkers while they encapsulated epoxy resin-based healing agents within the alginate shell via the electrospray method [33].

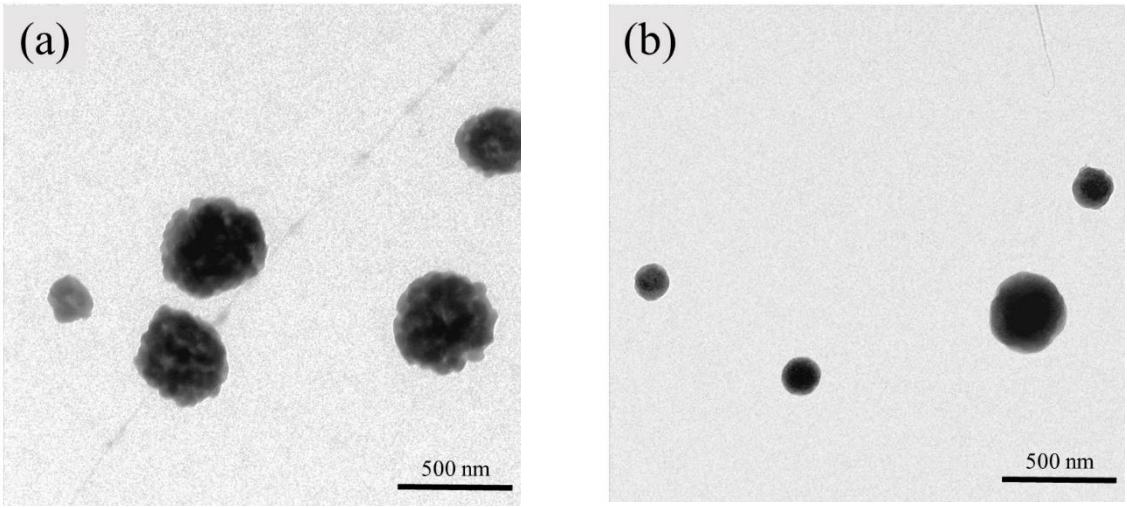

Figure 4. TEM images of the electrosprayed microcapsules (**a**) amine-containing capsules; (**b**) Isocyanate containing capsules.

3.2. Chemical structure of the Microcapsules

FTIR tests were carried out to make sure that no chemical reaction occurred between core and shell constituting materials during the encapsulation process. It should be noted that

the obtained microcapsules were washed with methanol and dried at 40 ℃ in a vacuum oven, before being crushed for testing. Figures 5a and 5b show the FTIR spectra of these two different core/shell materials. Figure 5a shows the FTIR spectra of the neat SAN microcapsules, neat amine, and crushed core-shell microcapsules. In the case of neat SAN, the FTIR spectrum shows the absorbance peak at 3085-3029 cm^{-1} which are attributed to the aromatic C–H stretching vibrations of the styrene ring. The band at 2924 cm^{-1} represents the aliphatic C–H stretching mode. The peak at 2238 cm^{-1} corresponds to the C≡N stretching of the nitrile group in the copolymer, and the peak at 1452 cm−1 is related to the bending of C–H bridging linkers [37].

The core material (amine terminated polyether) shows the aliphatic primary amine stretching vibration at 3370 cm^{-1} whose low intensity is due to the low concentration of the end-chain functional group in comparison with the repeating units. The absorbance bands at 2965, 2870, 1590 and 1455 cm^{-1} are attributed to the stretching vibrations of –CH2–, N–H and C–H groups, respectively [38]. The strong characteristic band at 1101 cm^{-1} is related to the aliphatic ether of the Polyetheramine chain. Regarding the core/shell microcapsules spectrum, the presence of core and shell characteristic peaks together proves the co-existence of both pristine materials in the prepared microcapsules without any harmful reactions. In particular, the presence of the two main peaks at 1101 and 3370 cm^{-1} attributable to the core material (marked with green color in Figure 5a) as well as the characteristic peaks of the shell component (marked with pink color in Figure 5a) in the microcapsules' spectrum confirms the encapsulation.

Similarly, Figure 5b shows the FTIR spectra of the neat isocyanate and of the related crushed microcapsules (together with that of neat SAN, for sake of comparison). The core material (*i.e.*, isocyanate) showed the N–H stretching vibration at 3392 cm^{-1}that is attributed to the polyurethane linkage between the isocyanate prepolymer segments. The strong stretching peak at 2274 cm^{-1} is related to the free isocyanate groups. The absorbance bands at

1720, 1521 and 1290 cm^{-1} are attributed to the stretching vibrations of –C=O, –NCO and C–N groups, respectively. Regarding to the core/shell microcapsules spectrum, the presence of core main peaks (marked with green color in Figure 5b) as well as the shell characteristic peaks (marked with pink color in Figure 5b) in the microcapsules spectrum confirms, again, the success of the encapsulation without any harmful reaction between the two main components. The peaks at2274 cm^{-1} of isocyanate and the 2237 cm^{-1} absorbance of acrylonitrile are the main proof for this.

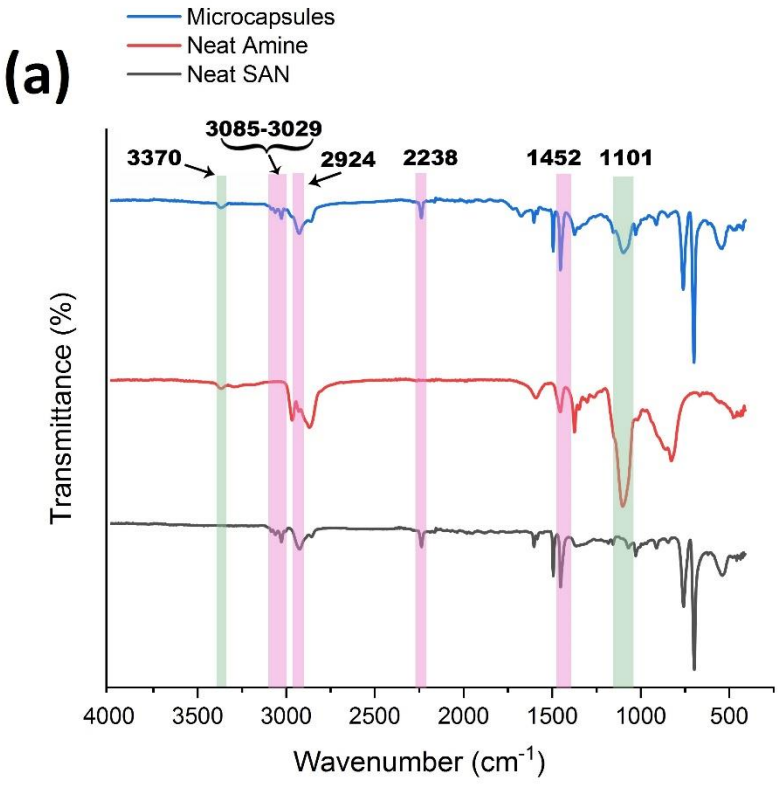

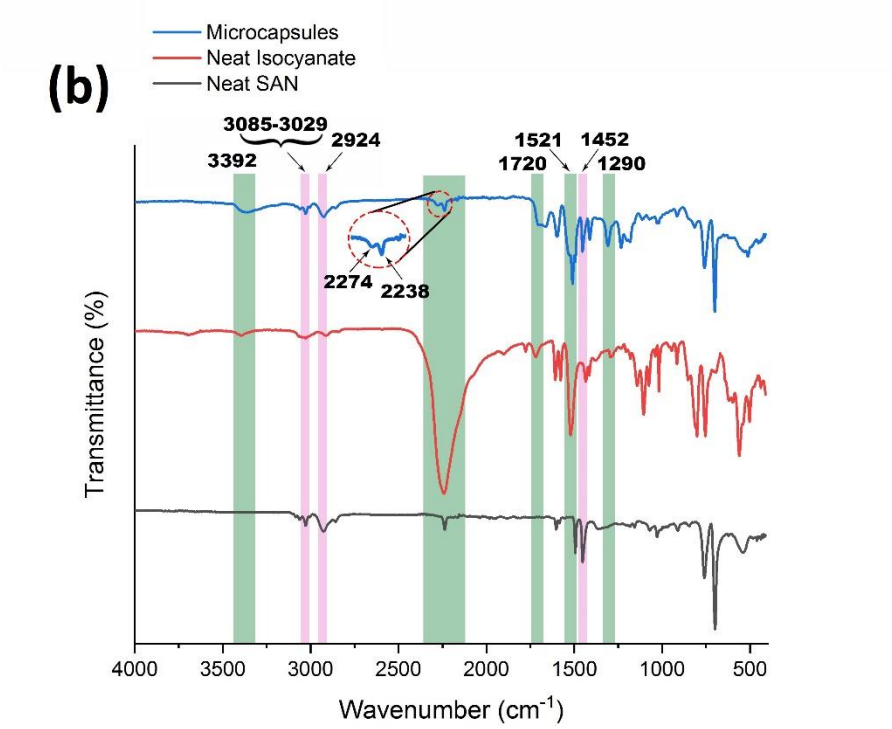

Figure 5. FTIR spectra of (**a**) neat SAN microcapsules, neat amine, and core-shell microcapsules containing amine; (**b**) neat SAN microcapsules, neat isocyanate, and core-shell microcapsules containing isocyanate.

3.3. Thermal stability of the microcapsules and encapsulation yield

Figure 6a and b show the TGA curves and the related differential ones (DTGA) of the amine-containing microcapsules as well as their single components. As ~~it~~ can be seen, the SAN shell is thermally stable up to 390 °C and then decomposes majorly at 440 °C, but there are still small residues of the acrylonitrile and styrene sections which start to decompose at higher temperatures [39]. In the case of pristine amine (*i.e.*, core), a two-stage thermal decomposition process occurred, starting at 120 °C and ending at 270 °C, tentatively attributed to the decomposition or evaporation of lower and higher molecular weight polyetheramine chains, respectively.

SAN/amine microcapsules showed a thermal decomposition behavior between those acquired for neat SAN and amine, confirming the presence of two types of materials in the microcapsules [37]. More in detail, the thermogram of the microcapsules shows all the three

processes. As better seen from DTGA curves (Figure 6b), the first and second stages overlap with those of the core material (amine) while the third stage is attributed to the shell polymer thermal decomposition.

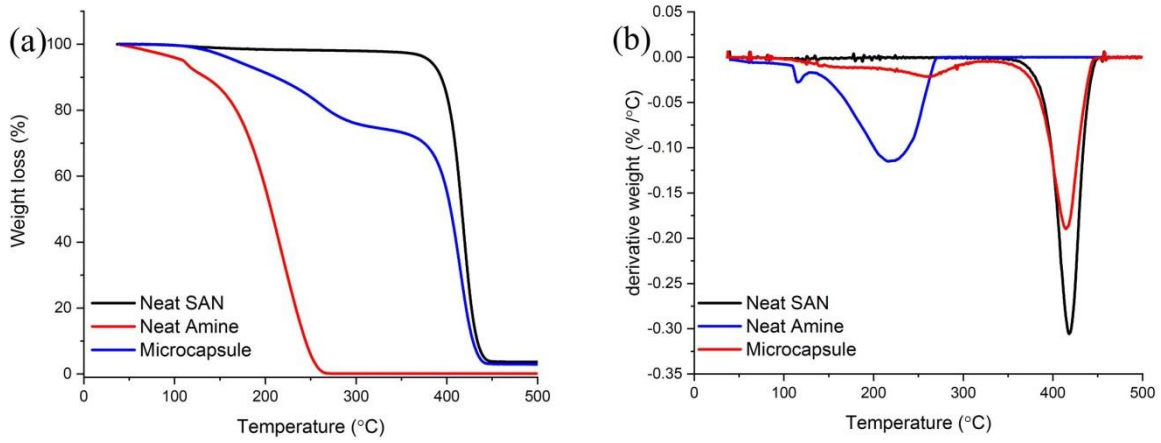

Figure 6. Thermogravimetric analysis of neat SAN microcapsules, neat amine, and related core-shell microcapsules under a nitrogen atmosphere, (**a**) TGA curves; (**b**) DTGA curves.

Similarly, Figures 7a and 7b present the same analysis for the isocyanate-containing microcapsules. It can be seen that the neat isocyanate shows one stage decomposition starting at 180 °C and terminating at 340 °C. The microcapsules show a two-stage decomposition attributed to isocyanate (core) and SAN (shell), respectively.

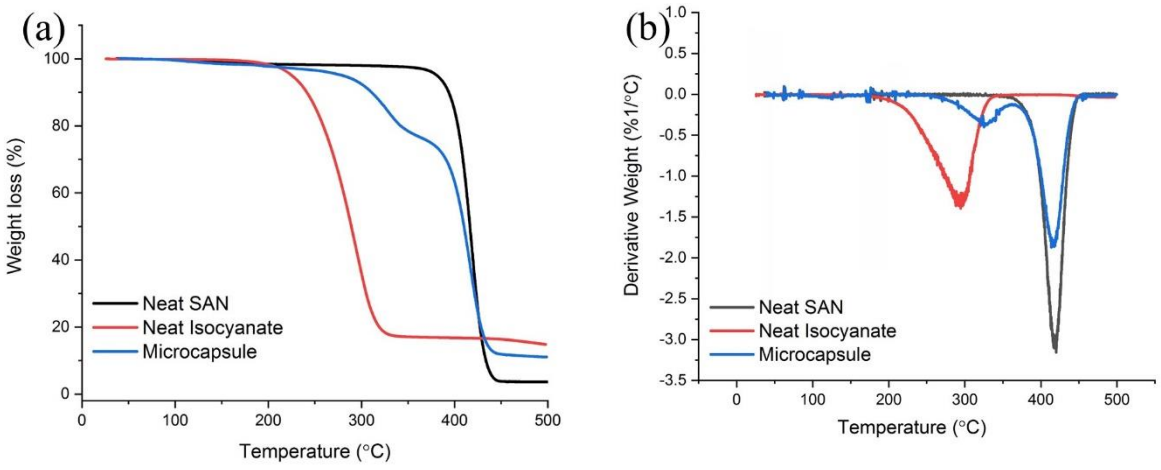

Figure 7. Thermogravimetric analysis of neat SAN microcapsules, neat isocyanate, and related core-shell microcapsules, (**a**) TGA curves; (**b**) DTGA curves.

The encapsulation process yield was calculated through the Eq. (1) [40]:

$$\%\alpha=[\%W_{core\text{-}exp}/\%W_{core\text{-}in}] \times 100, \quad (1)$$

In the above equation, α is the encapsulation yield, $\%W_{core\text{-}exp}$ is weight percent of the core material calculated from the TGA results and $\%W_{core\text{-}th}$ is the weight percent of the core material used in the encapsulation process, calculated as in Eq. (2):

$$\%W_{core\text{-}th} =[W_{core}/(W_{core}+W_{shell})] \times 100, \quad (2)$$

In Eq. (2) W_{shell} and W_{core} are the weight of shell and core materials used for the preparation of the initial polymer solution, respectively. The calculated values of the core contents and encapsulation yield are reported in Table 1. Encapsulation yield percentages for both cores are approximately 70%, in good agreement with the most successful and well studied conventional encapsulation methods [24, 41].

Table 1. The obtained core contents and encapsulation yields from TGA analyses.

	$\%W_{core\text{-}th}$	$\%W_{core\text{-}exp}$	%α
Amine containing microcapsules	33	23.5	71.2
Isocyanate containing microcapsules	33	22.5	68.1

3.4. Assessment of the healing reaction through electrochemical tests.

Figure 8 and Figure 9 represent the Bode modulus plot and Nyquist diagram of the samples resulted from electrochemical impedance spectroscopy. The diameter of the resulted semicircle in each Nyquist diagram corresponds to the charge transfer resistance (R_{ct}) associated with the corrosion process occurring at the metal|solution interface. As a consequence, R_{ct} is one of the key parameters useful to evaluate the barrier properties of a protective coating. According to Ohm's Law, R_{ct} is related inversely to the current density representing the corrosion reaction speed in electrochemical terms. According to this, the

sample with the largest semicircle diameter in the Nyquist plot has the highest resistance against corrosion. On the other hand, the Bode modulus plots represent the total impedance as a function of the frequency. The impedance value at the highest and lowest frequencies are attributed to the solution resistance and the total system resistance, respectively [42]. The last term is the sum of all resistive contributions of the studied system that, according to the equivalent circuit in Figure 10, also includes the coating resistance (R_{coat}) directly related to the porosity of the coating.

Figure 8 shows the EIS spectra for the cross-scratched control coating (capsule-free) and samples containing a total capsule content of 1 wt.%, after 14 days of exposition to a naturally aerated 3.5 wt.% NaCl solution. In order to evaluate the efficiency of the reaction between amine and isocyanates a dual capsule self-healing system, samples containing 1% of amine, 1% of isocyanate and 1% of the mixture (0.5% amine + 0.5% isocyanate) are compared. As can be seen in Figure 8a, the control sample exhibits a semicircle with the lowest diameter which is proof of the lowest resistance to corrosion reaction.The addition of the microcapsules has invariably increased the resistance of the coated samples. Sample with isocyanate microcapsules has a higher charge transfer resistance than the sample with amine one because of the fact that isocyanates can react also with the water during immersion and proceed a post healing [41]. The sample with the dual capsule system, which contains both amine and isocyanate microcapsules, has the highest resistance due to the synergetic polyurea formation reaction between the core reagents of the dual microcapsule system. Polyurea formation results in faster healing of the scratch and, as a consequence, a lower portion of metal is exposed to the corrosive environment.

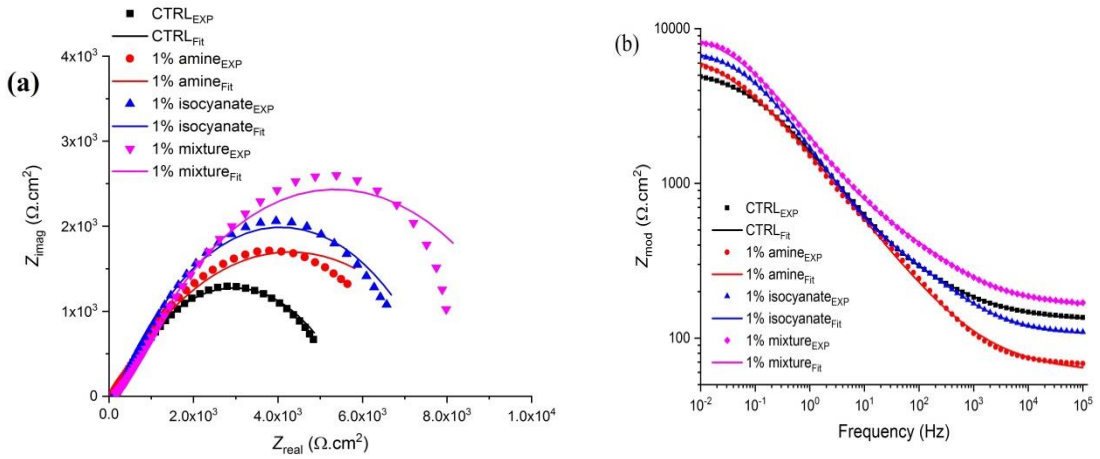

Figure 8. Electrochemical impedance spectroscopy spectra recorded at OCP for the scratched epoxy coatings after 14 days of aging into 3.5 wt.% NaCl solution, including the capsule-free control sample (black) and samples containing a total capsule content of 1 wt.%: (**a**) Nyquist diagrams; (**b**) Bode modulus plots. Full dots are the experimental data, while lines are the fitted spectra.

The effect of the total microcapsule content on the corrosion resistance of the coatings is also studied by EIS. Figure 9 shows the results for coatings containing 1, 2, 3 and 6 wt.% of microcapsules (keeping constant to 1:1 the amine to isocyanate microcapsules ratio). According to Figure 9, increasing the total microcapsule content increased the charge transfer resistance; the relation got reverse for the sample containing more than 3 wt.% of microcapsules. This decrease may be due to the agglomeration of microcapsules as well as the increased porosity caused by the presence of microcapsules in the coating matrix[19].

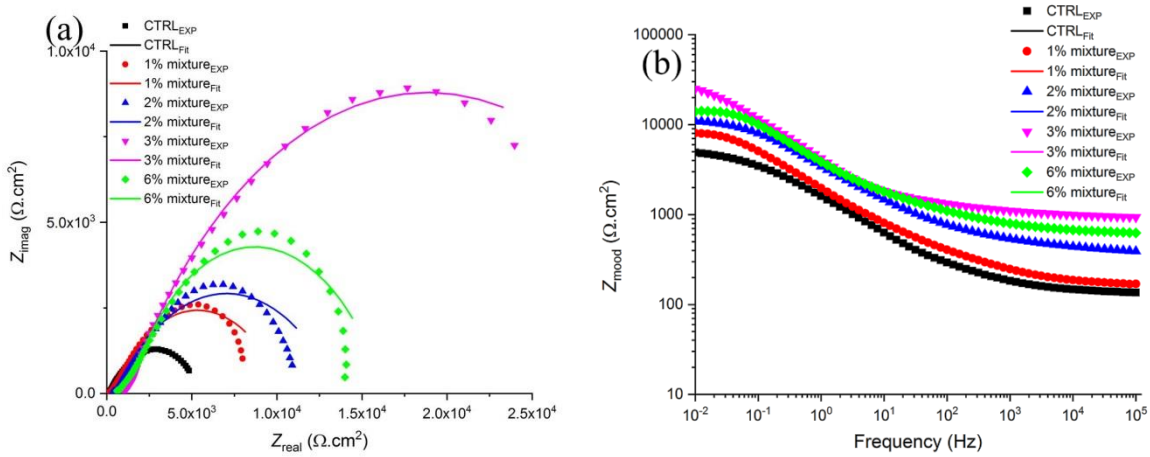

Figure 9. Electrochemical impedance spectroscopy spectra recorded at OCP for the scratched epoxy coatings including the control sample without microcapsule (black) and "dual capsule system" samples containing a total capsule content of 1, 2, 3 and 6 wt.% : (**a**) Nyquist diagrams; (**b**) Bode

modulus plots. Tests were performed after 14 days of aging into 3.5 wt.% NaCl solution. Full dots are the experimental data, while lines are the fitted spectra.

Fig 10 shows the electrical equivalent circuit which was used to fit the EIS data. It is a two-time constant circuit, commonly used in the analysis of metal surfaces covered with insulating coatings (*e.g.*, paint).

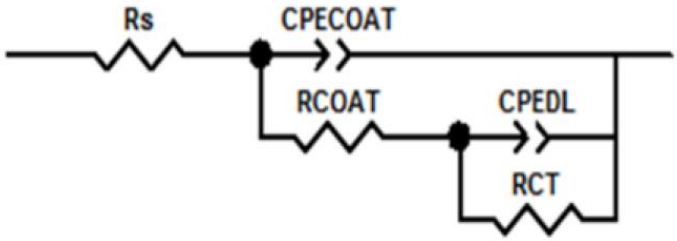

Figure 10. The electrical equivalent circuit utilized to analyze the EIS data.

Rs, Rcoat, Rct, CPEcoat, and CPEdl stand for solution resistance, coating resistance, charge transfer resistance, coating capacitance, and double layer capacitance, respectively. Constant phase element (CPE) was used instead of a capacitor to take into account the inhomogeneity of both coating and metal surfaces. The data calculated through this model by Gamry Echem Analyst software are summarized in Table 2.

Table 2. The EIS parameters of the scratched epoxy coatings including control coating and samples containing different kinds and amounts of microcapsules.

Sample	Rs ($\Omega.cm^2$)	Rcoat ($\Omega.cm^2$)	Rctr ($\Omega.cm^2$)	CPEcoat-Yo ($s^n.\Omega^{-1}.cm^{-2}$)	CPEcoat-α	CPEdl-Yo ($s^n.\Omega^{-1}.cm^{-2}$)	CPEdl-α
CTRL	130.1	274.7	5.35E+03	1.24E-04	5.28E-01	7.89E-05	5.79E-01
1%amine	69.2	755.1	6.24E+03	8.12E-05	6.22E-01	1.84E-04	5.87E-01
1%isocyanate	104.2	394.5	7.42E+03	7.80E-05	5.70E-01	1.10E-04	6.40E-01
1%mixture	158.5	697.6	9.61E+03	9.04E-05	5.19E-01	9.03E-05	6.34E-01
2%mixture	300.2	246.2	1.31E+04	1.16E-05	5.01E-01	8.51E-05	5.38E-01
3%mixture	885.3	545.8	3.61E+04	3.58E-05	4.78E-01	6.02E-05	6.55E-01
6%mixture	622.4	725.3	1.56E+04	1.74E-05	6.07E-01	7.17E-05	6.22E-01

The self-healing process produces a new polymer film in the scratched area. The corrosion is done by the diffusion of ions and oxygen through this new layer. According to the model data, Rct which is considerably higher than other resistances and similar to the resistance achieved experimentally in Bode modulus plot at low frequencies could be a good

sign for the ability of ions to reach the metal surface and, as a consequence, for the healing efficacy of the film. As it was clear from the Nyquist plots the 3% mixture sample has the highest resistance (Rct) among the others. Confirming the previous results, the Rct has increased by using the dual capsule system instead of the single one as well as increasing the total microcapsule content up to 3 % by weight. The highest Rct is 3.61E+04 for the "3%mixture " sample and the lowest Rct is 5.35E+03for the control sample. These results can be used to measure healing efficiency (HE) as follows [43, 44]:

$$\%HE = (1- Rct_0/Rct) \times 100, \quad (3)$$

Rct_0 and Rct are the charge transfer resistances of the neat coating (*i.e.,* capsule-free control sample) and the self-healing one, respectively.

The healing efficiency of 85.1% for the "3%mixture " sample confirms the performance of polyurea based dual capsule self-healing system in corrosion-resistant coatings.

According to the fact that the self-healing process is conducted via an extrinsic system, the effect of adding microcapsules to the coating matrix was studied by potentiodynamic polarization. It should be noted that in this case the coatings had no cracks and the microcapsules are present just as fillers in the matrix [45]. Figure 11a shows the potentiodynamic polarization curves for the pristine control coating and samples containing different microcapsule contents after 5 days of immersion in naturally aerated near-neutral 3.5 wt.% NaCl solution. According to the corrosion potential (E_{corr}) and the corrosion current density (i_{corr}) for each sample, it is clear that adding the microcapsules and increasing their amount increases the i_{corr} and shift the E_{corr} to more negative potentials. Both phenomena are representing a faster corrosion rate and a lower resistance against corrosion, respectively[19].

Potentiodynamic polarization analysis was also used to study the self-healing behavior of the cracked samples after 14 days of immersion in 3.5 wt.% NaCl solution. The pH of all

solutions after the immersion time was near neutral (6.5±0.3), practically the same value of the fresh solution. In these conditions, corrosion is supported cathodically by oxygen reduction. Oxygen must be transferred to the metal surface and adsorbed on it to react. As it can be seen in Figure 11b the polarization curve exhibits a limiting diffusion current density in the first part of the cathodic branch for all samples. Within this potential range, the diffusion is the rate-determining step of the process [46]. The limiting diffusion current density decreases with increasing the total capsule content up to 3 wt.%, while it increases for the 6 wt.% sample. For the more resistive coatings the surface in contact with the solution has decreased by the insulating film produced by the healing reaction, but in the 6% sample agglomeration of particles made the coating more porous and hence a wider contact surface between underlying metal and solution is expected. These results are qualitatively in good agreement with the behavior trend discussed with the EIS results.

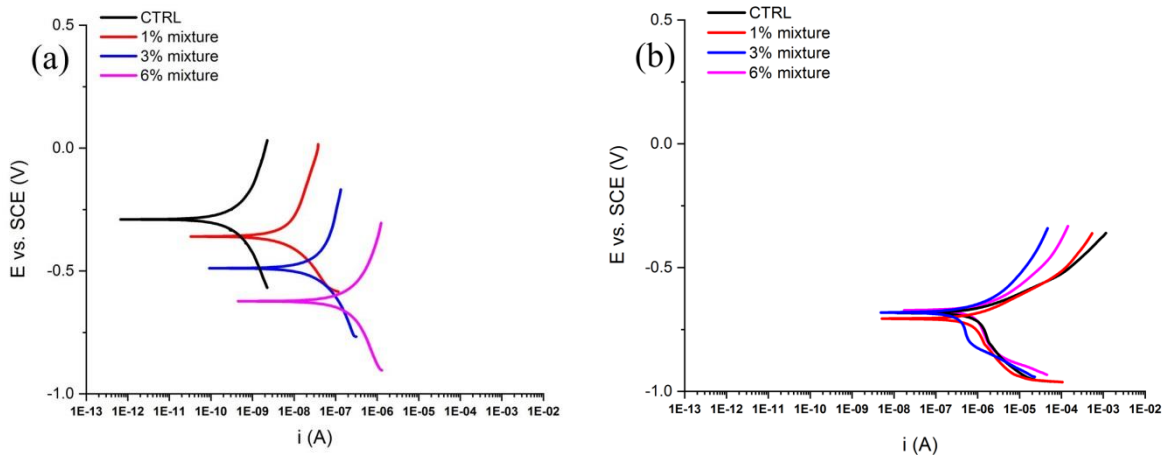

Figure 11. Potentiodynamic polarization curves for the control coating and samples containing different microcapsule contents: (**a**) coatings without a scratch and immersed for 5 days in 3.5 wt.% NaCl solution; (**b**) coatings with cross-scratch and immersed for 14 days in 3.5 wt.% NaCl solution. sweep rate potential: 0.167 mV s^{-1}.

4. Conclusions

A facile strategy was utilized to develop dual capsule self-healing epoxy coatings. A hydrophilic polyetheramine and a highly reactive MDI-based isocyanate were successfully encapsulated within poly(styrene-co-acrylonitrile) shell by a single step electrospray process.

The encapsulation yield was 71.2% and 68.1%, respectively. The mean diameter of the resulted microcapsules for both core materials was lower than 2 μm. EIS and potentiodynamic polarization techniques were used to evaluate the self-healing system performance in an epoxy anti-corrosion coating for steel. Results showed that amine and isocyanate-containing microcapsules co-present into the coating assure a good performance due to the synergetic polyurea formation reaction between the core reagents of this dual microcapsule system formulation. Increasing the total content of microcapsules up to 3 wt.% increased the corrosion resistance of the coating but this relation got reverse for the sample containing 6 wt.%. This phenomenon is due to the microcapsules agglomeration and the related increased porosity of the coating matrix, as confirmed by potentiodynamic polarization tests on intact (*i.e.*, scratch-free) samples. The EIS results were modeled by a proper electrical equivalent circuit to estimate the healing efficiency. The highest healing efficiency of 85.1% was achieved with the "3%mixture " sample. These results confirmed the promising performance of a polyurea-based dual capsule self-healing system in the development of corrosion-resistant coatings.

Acknowledgments: The authors express their sincere gratitude to the Iranian Ministry of Science, Research and Technology (MSRT) for the monetary support of a research visit to Università degli Studi di Milano for the accomplishment of this work. This work was also supported through a grant from the Iran National Science Foundation (INSF, Grant No. 97008660).

References

[1] Koch G, Varney J, Thompson N, Moghissi O, Gould M and Payer J 2016 International measures of prevention, application, and economics of corrosion technologies study *NACE International*

[2] Sørensen P A, Kiil S, Dam-Johansen K and Weinell C E 2009 Anticorrosive coatings: a review *Journal of Coatings Technology and Research* **6** 135-76

[3] Forsgren A and Knudsen O Ø 2017 *Corrosion control through organic coatings*: CRC Press)

[4] Lyon S B, Bingham R and Mills D J 2017 Advances in corrosion protection by organic coatings: What we know and what we would like to know *Progress in Organic Coatings* **102** 2-7

[5] Ghauri F A, Raza M A, Baig M S and Ibrahim S 2017 Corrosion study of the graphene oxide and reduced graphene oxide-based epoxy coatings *Materials Research Express* **4** 125601

[6] Nawaz M, Yusuf N, Habib S, Shakoor A R, Ubaid F, Ahmad Z, Kahraman R, Mansour S and Gao W 2019 Development and Properties of Polymeric Nanocomposite Coatings *Polymers* **11**

[7] Blaiszik B J, Kramer S L, Olugebefola S C, Moore J S, Sottos N R and White S R 2010 Self-healing polymers and composites *Annual Review of Materials Research* **40** 179-211

[8] Aïssa B 2014 *Self-healing Materials: Innovative Materials for Terrestrial and Space Applications*: Smithers Rapra)

[9] White S R, Sottos N, Geubelle P, Moore J, Kessler M R, Sriram S, Brown E and Viswanathan S 2001 Autonomic healing of polymer composites *Nature* **409** 794

[10] Zhang M Q and Rong M Z 2011 *Self-healing polymers and polymer composites*: John Wiley & Sons)

[11] Vijay Kumar V, Balaganesan G, Lee J K Y, Neisiany R E, Surendran S and Ramakrishna S 2019 A Review of Recent Advances in Nanoengineered Polymer Composites *Polymers* **11** 644

[12] Mphahlele K, Ray S S and Kolesnikov A 2017 Self-Healing Polymeric Composite Material Design, Failure Analysis and Future Outlook: A Review *Polymers* **9**

[13] Zhang G, Pei J, Li R, Li P and Zhou B 2018 The preparation and characterization of a novel self-healing based on the dynamic translocation of disulfide bonds *Materials Research Express* **5** 105301

[14] Dai S, Wang S, Yan H, Xu J, Hu H, Ding J and Yuan N 2019 Stretchable and self-healable hydrogel-based capacitance pressure and strain sensor for electronic skin systems *Materials Research Express* **6** 0850b9

[15] Khoee S, Payandeh S H, Jafarzadeh P and Asadi H 2016 Size and core content optimization of epoxy nanocapsules by response surface methodology for use in self-healing coatings *Smart Materials and Structures* **25** 084014

[16] Zwaag S 2008 *Self healing materials: an alternative approach to 20 centuries of materials science* vol 30: Springer Science+ Business Media BV)

[17] Hillewaere X K and Du Prez F E 2015 Fifteen chemistries for autonomous external self-healing polymers and composites *Progress in Polymer Science* **49** 121-53

[18] Safaei F, Khorasani S N, Rahnama H, Neisiany R E and Koochaki M S 2018 Single microcapsules containing epoxy healing agent used for development in the fabrication of cost efficient self-healing epoxy coating *Progress in Organic Coatings* **114** 40-6

[19] Ataei S, Khorasani S N, Torkaman R, Neisiany R E and Koochaki M S 2018 Self-healing performance of an epoxy coating containing microencapsulated alkyd resin based on coconut oil *Progress in Organic Coatings* **120** 160-6

[20] Kim D-M, Cho Y-J, Choi J-Y, Kim B-J, Jin S-W and Chung C-M 2017 Low-Temperature Self-Healing of a Microcapsule-Type Protective Coating *Materials* **10** 1079

[21] Brown E N, Kessler M R, Sottos N R and White S R 2003 In situ poly (urea-formaldehyde) microencapsulation of dicyclopentadiene *Journal of microencapsulation* **20** 719-30

[22] Cho S H, Andersson H M, White S R, Sottos N R and Braun P V 2006 Polydimethylsiloxane-based self-healing materials *Advanced Materials* **18** 997-1000

[23] González L, Kostrzewska M, Baoguang M, Li L, Hansen J H, Hvilsted S and Skov A L 2014 Preparation and characterization of silicone liquid core/polymer shell microcapsules via internal phase separation *Macromolecular Materials and Engineering* **299** 1259-67

[24] McIlroy D A, Blaiszik B J, Caruso M M, White S R, Moore J S and Sottos N R 2010 Microencapsulation of a reactive liquid-phase amine for self-healing epoxy composites *Macromolecules* **43** 1855-9

[25] Vijayan P and AlMaadeed M 2016 'Containers' for self-healing epoxy composites and coating: Trends and advances *Express Polymer Letters* **10**

[26] Mutlu E C, Ficai A, Ficai D, Yildirim A B, Yildirim M, Oktar F N and Demir A 2018 Chitosan/poly (ethylene glycol)/hyaluronic acid biocompatible patches obtained by electrospraying *Biomedical Materials* **13** 055011

[27] Mutlu E C, Yıldırım A B, Yıldırım M, Ficai A, Ficai D, Oktar F N, Ţîţu M, Çetinkaya A and Demir A 2019 Improvement of antibacterial and biocompatibility properties of electrospray biopolymer films by ZnO and MCM-41 *Polymer Bulletin* 1-19

[28] Park J H and Braun P V 2010 Coaxial electrospinning of self-healing coatings *Advanced materials* **22** 496-9

[29] Sinha-Ray S, Pelot D, Zhou Z, Rahman A, Wu X-F and Yarin A 2012 Encapsulation of self-healing materials by coelectrospinning, emulsion electrospinning, solution blowing and intercalation *Journal of Materials Chemistry* **22** 9138-46

[30] Hansen C J, Wu W, Toohey K S, Sottos N R, White S R and Lewis J A 2009 Self-healing materials with interpenetrating microvascular networks *Advanced Materials* **21** 4143-7

[31] Vahedi V, Pasbakhsh P, Piao C S and Seng C E 2015 A facile method for preparation of self-healing epoxy composites: using electrospun nanofibers as microchannels *Journal of Materials Chemistry A* **3** 16005-12

[32] Neisiany R E, Khorasani S N, Lee J K Y and Ramakrishna S 2016 Encapsulation of epoxy and amine curing agent in PAN nanofibers by coaxial electrospinning for self-healing purposes *RSC Advances* **6** 70056-63

[33] Hia I L, Pasbakhsh P, Chan E-S and Chai S-P 2016 Electrosprayed multi-core alginate microcapsules as novel self-healing containers *Scientific reports* **6** 34674

[34] Zhou S, Wu Y, Zhao W, Yu J, Jiang F and Ma L 2018 Comparative corrosion resistance of graphene sheets with different structures in waterborne epoxy coatings *Colloids and Surfaces A: Physicochemical and Engineering Aspects* **556** 273-83

[35] Primeaux D J 2004 Polyurea elastomer technology: history, chemistry & basic formulating techniques *Primeaux Associates LLC* 1-20

[36] Broekaert M 2002 Polyurea spray coatings. The Technology and Latest Developments *Paint & Coatings Industry* **18** 80-2

[37] Neisiany R E, Lee J K Y, Khorasani S N and Ramakrishna S 2017 Towards the development of self-healing carbon/epoxy composites with improved potential provided by efficient encapsulation of healing agents in core-shell nanofibers *Polymer Testing* **62** 79-87

[38] Chen B, Li J, Liu T, Dai Z and Zhao H 2018 Facile preparation of epoxy based elastomers with tunable T gs and mechanical properties *RSC advances* **8** 13474-81

[39] Xue T J and Wilkie C A 1997 Thermal degradation of poly (styrene-g-acrylonitrile) *Polymer degradation and stability* **56** 109-13

[40] Yao L, Yuan Y C, Rong M Z and Zhang M Q 2011 Self-healing linear polymers based on RAFT polymerization *Polymer* **52** 3137-45

[41] Huang M and Yang J 2011 Facile microencapsulation of HDI for self-healing anticorrosion coatings *Journal of Materials Chemistry* **21** 11123-30

[42] Bakhshandeh E, Jannesari A, Ranjbar Z, Sobhani S and Saeb M R 2014 Anti-corrosion hybrid coatings based on epoxy–silica nano-composites: toward relationship between the morphology and EIS data *Progress in Organic Coatings* **77** 1169-83

[43] Atta A M, El-Azabawy O E, Ismail H and Hegazy M 2011 Novel dispersed magnetite core–shell nanogel polymers as corrosion inhibitors for carbon steel in acidic medium *Corrosion science* **53** 1680-9

[44] Atta A, El-Mahdy G, Al-Lohedan H and Al-Hussain S 2014 Synthesis of environmentally friendly highly dispersed magnetite nanoparticles based on rosin cationic surfactants as thin film coatings of steel *International journal of molecular sciences* **15** 6974-89

[45] Raps D, Hack T, Kolb M, Zheludkevich M and Nuyken O 2010 *Smart Coatings III*: ACS Publications) pp 165-89

[46] Jaggi S, Elsener B and Bohni H 2000 Oxygen reduction on mild steel and stainless steel in alkaline solutions *European Federation of Corrosion Publications(UK)* **31** 3-12